

Hot electron cooling in Dirac semimetal Cd₃As₂ due to polar optical phonons

Shrishail S. Kubakaddi* and Tutul Biswas†

*Department of Physics, K. L. E. Technological University, Hubballi-580 031, Karnataka, India

†Department of Physics, University of North Bengal, Raja Rammohunpur-734013, India

(Dated: August 13, 2018)

A theory of hot electron cooling power due to polar optical phonons P_{op} is developed in three-dimensional Dirac semimetal(3DDS) Cd₃As₂ taking account of hot phonon effect. Hot phonon distribution N_q and P_{op} are investigated as a function of electron temperature T_e , electron density n_e , and phonon relaxation time τ_p . It is found that P_{op} increases rapidly (slowly) with T_e at lower (higher) temperature regime. Whereas, P_{op} is weakly decreasing with increasing n_e . The results are compared with those for three-dimensional electron gas (3DEG) in Cd₃As₂ semiconductor. Hot phonon effect is found to reduce P_{op} considerably and it is stronger in 3DDS Cd₃As₂ than in Cd₃As₂ semiconductor. P_{op} is also compared with the hot electron cooling power due to acoustic phonons P_{ac} . We find that a crossover takes place from P_{ac} dominated cooling at low T_e to P_{op} dominated cooling at higher T_e . The temperature at which this crossover occurs shifts towards higher values with the increase of n_e . Also, hot electron energy relaxation time τ_e is discussed and estimated.

PACS numbers: 72.10.-d, 73.63.-b 73.20.-r

I. INTRODUCTION

Recently, theoretically predicted^{1,2} and by now experimentally realized and verified three-dimensional Dirac semimetals (3DDS) have become the rapidly growing field of research interest³⁻¹⁷. These 3DDS, the three-dimensional (3D) analogue of graphene, have gapless band feature with linear band dispersion and vanishing effective mass in their low energy states. The cadmium arsenide (Cd₃As₂), a potential representative of 3DDS, has drawn more attention as it is robust and chemically stable compound in air with ultrahigh mobility^{4,5,9,10}. The linear band picture of 3D Dirac fermions has lead 3DDS to exhibit many unusual transport phenomena such as strong quantum oscillations^{7,10}, ultrahigh mobility^{9,10,18} and giant magneto resistance^{9,18-20}. Besides, several promising applications of bulk Dirac fermions in Cd₃As₂ in photonic devices such as ultrafast broadband infrared photodetectors¹³ and ultrafast optical switching mechanism for the mid-infrared¹⁷ have been realized and demonstrated. Because of the inherent zero energy gap and linear band dispersion, 3DDS can absorb photons in the entire infrared region. These 3DDS have advantage over two-dimensional (2D) Dirac semimetals like monolayer graphene because bulk nature of 3DDS enhances the efficiency of photon absorption.

The experimentally reported low temperature (~ 5 K) high mobilities $\sim 9 \times 10^6$ cm²/V-s^{5,6,9,10} and up to 4.60×10^7 cm²/V-s¹⁰ are higher than that in suspended graphene. The measurements of resistivity ρ vs temperature T , show $\rho \sim T$ down to low T , which is inferred to be due to unklapp processes and electron-optical phonon scattering¹⁰. High quality 3DDS Cd₃As₂ microbelts²¹ and nanobelts²² with room temperature electron mobility $\sim 2 \times 10^4$ cm²/V-s have been fabricated. In nanobelt²², the Hall mobility μ_H follows the typical relation $\mu_H \sim T^{-\gamma}$ with $\gamma=0.5$, in the range 20-200 K, which is attributed to the enhanced electron-phonon (el-

ph) scattering.

Theoretically, electronic transport properties of 3D Weyl and Dirac semimetals are studied using the semiclassical Boltzmann transport equation^{23,24}. Considering the electron momentum relaxation processes due to scattering by disorder (short-range and long-range) and acoustic phonons, the latter is shown to dominate electrical conductivity at higher temperature²⁴. However, the quantitative comparison between the existing experimental results and theoretical calculations is still lacking.

In order to find the applications of 3DDS in devices operating in the high field region, it is important to investigate the steady state energy relaxation of the hot carriers, in these systems, by emission of phonons as the only cooling channel. In high electric field electrons gain energy and establish their 'hot electron temperature T_e ' which is greater than the lattice temperature T . In the steady state these hot electrons transfer their energy to lattice by emission of acoustic (optical) phonons at relatively low (high) temperature. The electron heating affects the device operation significantly, in the high field region, as it governs the thermal dissipation and heat management. To enhance the device efficiency, it is important to reduce the hot electron power loss.

The hot electron energy relaxation by emission of acoustic and optical phonons has been extensively investigated theoretically and experimentally in conventional 3D electron gas (3DEG) in bulk semiconductors²⁵⁻³¹, 2D electron gas (2DEG) in semiconductor heterostructures^{31,32}, monolayer graphene³³ and bilayer graphene³⁴. Recently, hot electron cooling is theoretically studied in monolayer MoS₂³⁵ and quasi-2DEG in gapped Cd₃As₂ film³⁶. There exist theoretical studies of hot 3D Dirac fermion cooling power due to electron-acoustic phonon interaction P_{ac} in Cd₃As₂^{37,38}. The deformation potential coupling constant D (~ 10 -30 eV)³⁹ determines the strength of electron-acoustic phonon scattering. In the Bloch-Grüneisen (BG) regime the power

laws of P_{ac} dependence on electron temperature T_e and electron density n_e are predicted³⁸.

Experimentally, the phonon mediated hot electron cooling of photoexcited carriers has been investigated in Cd_3As_2 from pump-probe measurements^{11,14-16}. The cooling process of photoexcited carriers is shown to be through emission of acoustic and optical phonons^{11,14}, with relatively low optical phonon energies ~ 25 meV^{14,40}. The hot electron cooling, apart from relating el-ph scattering to the high field transport properties, it also plays significant role in designing high speed electronic and photonic devices of Cd_3As_2 . Thus, el-ph interaction is a key issue and central to the understanding of devices based on Cd_3As_2 .

It is important to notice that, in 3DDS Cd_3As_2 , although there is strong experimental evidence of photoexcited hot carrier energy relaxation by optical phonon emission^{11,14,15}, the steady state hot electron cooling by emission of optical phonons has not been addressed both theoretically and experimentally. In the present work, we theoretically investigate the hot electron cooling power in 3DDS Cd_3As_2 by emission of optical phonons P_{op} including the hot phonon effect. Numerical results are obtained as a function of electron temperature, electron density and phonon relaxation time. These results are compared with P_{op} in bulk Cd_3As_2 semiconductor and with P_{ac} , in 3DDS Cd_3As_2 . This study is expected to provide thermal link between electrons and phonons in 3DDS Cd_3As_2 for its application in high speed/field devices.

The structure of the paper is shaped in the following way. In section II we provide all the theoretical ingredients including hot phonon effect, cooling power due to optical and acoustic phonons in 3DDS Cd_3As_2 , and cooling power for 3DEG in bulk Cd_3As_2 semiconductor. The obtained results are discussed in section III. Finally a summary of the present work is given in section IV.

II. THEORY

In this section we develop a theory for the cooling power of hot electrons in 3DDS mediated by polar optical phonons. For comparison purpose we shall also provide the results for cooling power due to acoustic phonon in 3DDS as well as that in bulk Cd_3As_2 semiconductor due to polar optical phonon. Let us start with mentioning the basic properties of the physical system chosen.

A. Preliminary informations

We consider the Dirac fermion gas in a 3DDS Cd_3As_2 in which the low energy excitations are described by the Dirac like linear dispersion $E_{\mathbf{k}} = s\hbar v_F|\mathbf{k}|$ in the long wavelength continuum limit. Here, v_F is the Fermi velocity, \mathbf{k} is the 3D electronic wave vector, and the band index s takes the value $+1(-1)$ for conduction(valence) band. The corresponding eigenstate is

given by $\psi_{\mathbf{k}}^s = (1/\sqrt{2V})e^{i\mathbf{k}\cdot\mathbf{r}}\chi^s$, where V is the volume of the system, $\chi^+ = [\cos(\theta/2) \ \sin(\theta/2)e^{i\phi}]^T$ and $\chi^- = [\sin(\theta/2) \ -\cos(\theta/2)e^{i\phi}]^T$ with θ and ϕ are the polar and azimuthal angle in three dimensional \mathbf{k} -space, respectively. The corresponding density of states is given by $D(E_{\mathbf{k}}) = gE_{\mathbf{k}}^2/(2\pi^2\hbar^3v_F^3)$, where $g = g_s g_v$ with $g_s(g_v)$ is the spin(valley) degeneracy.

B. Hot electron cooling power in 3DDS

In order to formulate a theory for the hot electron cooling power in 3DDS, we work in the ‘‘hot electron temperature model’’ in which the electron gas is assumed to be in equilibrium with itself at an elevated temperature T_e than the lattice temperature T . In this model Dirac fermions are assumed to have the usual Fermi-Dirac distribution $f(E_{\mathbf{k}}) = [\exp\{\beta_e(E_{\mathbf{k}} - \mu)\} + 1]^{-1}$ where $\beta_e = (k_B T_e)^{-1}$ and μ is the chemical potential determined by the electron density $n_e = \int f(E_{\mathbf{k}})D(E_{\mathbf{k}})dE_{\mathbf{k}}$. The 3D Dirac fermions are assumed to interact with the 3D phonons of energy $\hbar\omega_{\mathbf{q}}$ and wave vector \mathbf{q} . The cooling power per electron P (i.e. average electron energy loss rate) due to el-ph interaction can be obtained by using the well known technique described in Ref. [25]. It is given by

$$P = -\frac{1}{N_e} \sum_{\mathbf{q}} \hbar\omega_{\mathbf{q}} \left(\frac{dN_{\mathbf{q}}}{dt} \right)_{\text{el-ph}}, \quad (1)$$

where N_e is total number of electrons, $N_{\mathbf{q}}$ is the non-equilibrium phonon distribution function. The rate of change of $N_{\mathbf{q}}$ due to electron-phonon interaction i.e. $(dN_{\mathbf{q}}/dt)_{\text{el-ph}}$ is given by using Fermi's golden rule

$$\begin{aligned} \left(\frac{dN_{\mathbf{q}}}{dt} \right)_{\text{el-ph}} &= \frac{2\pi g}{\hbar} \sum_{\mathbf{k}} |M(\mathbf{q})|^2 \left\{ (N_{\mathbf{q}} + 1) f(E_{\mathbf{k}} + \hbar\omega_{\mathbf{q}}) \right. \\ &\times [1 - f(E_{\mathbf{k}})] - N_{\mathbf{q}} f(E_{\mathbf{k}}) [1 - f(E_{\mathbf{k}} + \hbar\omega_{\mathbf{q}})] \left. \right\} \\ &\times \delta(E_{\mathbf{k}+\mathbf{q}} - E_{\mathbf{k}} - \hbar\omega_{\mathbf{q}}), \end{aligned} \quad (2)$$

where $|M(\mathbf{q})|^2 = |g(q)|^2 |F(\theta_{\mathbf{k},\mathbf{k}'})|^2$ is the square of the matrix element for the el-ph interaction. Here, $|g(q)|^2$ is square of el-ph matrix element without chiral wave function and $|F(\theta_{\mathbf{k},\mathbf{k}'})|^2 = (1 + \cos \theta_{\mathbf{k},\mathbf{k}'})/2$ with $\theta_{\mathbf{k},\mathbf{k}'}$ being the angle between \mathbf{k} and \mathbf{k}' , resulting from the chiral nature of the Dirac fermion.

One may also write Eq.(2) in the following form

$$\left(\frac{dN_{\mathbf{q}}}{dt} \right)_{\text{el-ph}} = \left[(N_{\mathbf{q}} + 1) e^{-\beta_e \hbar\omega_{\mathbf{q}}} - N_{\mathbf{q}} \right] \Gamma_{\mathbf{q}}, \quad (3)$$

where $\Gamma_{\mathbf{q}}$ is given by

$$\begin{aligned} \Gamma_{\mathbf{q}} &= \frac{2\pi g}{\hbar} \sum_{\mathbf{k}} |M(\mathbf{q})|^2 f(E_{\mathbf{k}}) [1 - f(E_{\mathbf{k}} + \hbar\omega_{\mathbf{q}})] \\ &\times \delta(E_{\mathbf{k}+\mathbf{q}} - E_{\mathbf{k}} - \hbar\omega_{\mathbf{q}}). \end{aligned} \quad (4)$$

As a result the cooling power(Eq. (1)) becomes

$$P = \frac{1}{N_e} \sum_{\mathbf{q}} \hbar\omega_{\mathbf{q}} [(N_{\mathbf{q}} + 1)e^{-\beta_e \hbar\omega_{\mathbf{q}}} - N_{\mathbf{q}}] \Gamma_{\mathbf{q}}. \quad (5)$$

Our objective is to find hot electron cooling power P_{op} due to optical phonons. The optical phonon energy $\hbar\omega_{\mathbf{q}} = \hbar\omega_0$ is taken to be constant. The summation over \mathbf{q} in Eq. (5) can be converted into integral as $\sum_{\mathbf{q}} \rightarrow (V/8\pi^3) \int_0^\infty q^2 dq \int_0^\pi \sin \varphi d\varphi \int_0^{2\pi} d\psi$ with φ and ψ are the polar and azimuthal angle of \mathbf{q} , respectively. Note that the integrations over φ and ψ give 4π . Defining $E_q = \hbar v_F q$, we find hot electron cooling power as

$$P_{\text{op}} = \frac{\hbar\omega_0}{2\pi^2 n_e \hbar^3 v_F^3} \int_0^\infty dE_q E_q^2 [(N_q + 1)e^{-\beta_e \hbar\omega_0} - N_q] \Gamma_q. \quad (6)$$

An explicit evaluation of Γ_q is given in the section II(D).

C. Hot phonon distribution

Non-equilibrium phonon distribution $N_{\mathbf{q}}$ can be obtained from the Boltzmann equation

$$\left(\frac{dN_{\mathbf{q}}}{dt} \right)_{\text{el-ph}} + \left(\frac{dN_{\mathbf{q}}}{dt} \right)_{\text{oth}} = 0, \quad (7)$$

where the first term describes the rate of change of the phonon distribution due to electron-phonon interaction while the later one denotes the same due to the other processes namely phonon-phonon interaction, surface roughness scattering etc.

In the relaxation time approximation one can write

$$\left(\frac{dN_{\mathbf{q}}}{dt} \right)_{\text{oth}} = -\frac{N_{\mathbf{q}} - N_{\mathbf{q}}^0}{\tau_p}, \quad (8)$$

where, $N_{\mathbf{q}}^0 = [\exp(\beta \hbar\omega_0) - 1]^{-1}$ with $\beta = (k_B T)^{-1}$ is the phonon distribution at equilibrium and τ_p is phonon relaxation time due to all other mechanisms.

Hence, the non-equilibrium phonon distribution $N_{\mathbf{q}}$ will be readily obtained from Eq.(7) as

$$N_{\mathbf{q}} = N_{\mathbf{q}}^0 + \tau_p \left(\frac{dN_{\mathbf{q}}}{dt} \right)_{\text{el-ph}}. \quad (9)$$

Inserting Eq. (3) into Eq. (9) and considering $\hbar\omega_{\mathbf{q}} = \hbar\omega_0$, we find $N_{\mathbf{q}}$ as

$$N_{\mathbf{q}} = \frac{N_{\mathbf{q}}^0 + \tau_p \Gamma_{\mathbf{q}} e^{-\beta_e \hbar\omega_0}}{1 + \tau_p \Gamma_{\mathbf{q}} (1 - e^{-\beta_e \hbar\omega_0})}. \quad (10)$$

D. Evaluation of Γ_q

Here, we shall provide an explicit evaluation of el-ph scattering rate Γ_q . We assume the electron-optical

phonon interaction via Fröhlich coupling with the corresponding matrix element $|g(q)|^2 = 2\pi e^2 \hbar\omega_0 (\varepsilon_\infty^{-1} - \varepsilon_0^{-1}) / (Vq^2)$, where $\varepsilon_\infty(\varepsilon_0)$ is the high frequency (static) dielectric constant of the material. Momentum conservation $\mathbf{k}' = \mathbf{k} + \mathbf{q}$ also allow us to write $|F(\theta_{\mathbf{k},\mathbf{k}'})|^2$ as

$$|F(\theta_{\mathbf{k},\mathbf{k}+\mathbf{q}})|^2 = \frac{1}{2} \left(1 + \frac{E_k + E_q \cos \theta}{E_k + \hbar\omega_0} \right). \quad (11)$$

Converting the summation over \mathbf{k} into integrals like $\sum_{\mathbf{k}} \rightarrow V/((2\pi)^3) \int dk k^2 \sin \theta d\theta d\phi$, Eq.(4) becomes

$$\Gamma_{\mathbf{q}} = \frac{2\pi g}{\hbar} \frac{V}{(2\pi)^3} \int k^2 dk dx d\phi |g(q)|^2 |F(\theta_{\mathbf{k},\mathbf{k}+\mathbf{q}})|^2 \times f(E_k) [1 - f(E_k + \hbar\omega_0)] \delta[X(x)], \quad (12)$$

where the argument of the delta function is

$$X(x) = (E_k^2 + E_q^2 + 2E_k E_q x)^{\frac{1}{2}} - E_k - \hbar\omega_0 \quad (13)$$

with $x \equiv \cos \theta$. Note that the ϕ -integral in Eq. (12) gives 2π since the integrand is independent of ϕ . The x -integral can be evaluated by the following property of the delta function

$$\delta[X(x)] = \frac{\delta(x - x_i)}{\left. \frac{dX}{dx} \right|_{x=x_i}}, \quad (14)$$

where the root x_i of Eq.(13) can be obtained as

$$x_i = \frac{(\hbar\omega_0)^2 + 2E_k \hbar\omega_0 - E_q^2}{2E_k E_q}. \quad (15)$$

Hence, after doing the angular integrations, Eq. (12) becomes

$$\Gamma_q = g \frac{V|g(q)|^2}{2\pi \hbar (\hbar v_F)^3 E_q} \int_{E_k^{\text{min}}}^\infty dE_k E_k |F(E_k, E_q)|^2 \times f(E_k) [1 - f(E_k + \hbar\omega_0)] (E_k + \hbar\omega_0), \quad (16)$$

where $E_k^{\text{min}} = (E_q - \hbar\omega_0)/2$. This lower limit of E_k -integral is a consequence of the fact that $-1 \leq x_i \leq 1$. Note also that

$$|F(E_k, E_q)|^2 = \frac{1}{2} \left[1 + \frac{(E_k + \hbar\omega_0)^2 + E_k^2 - E_q^2}{2E_k(E_k + \hbar\omega_0)} \right]. \quad (17)$$

E. Hot electron cooling power due to acoustic phonons in 3DDS

As we are giving results for hot electron cooling power P_{ac} due to acoustic phonons, for the sake of comparison with P_{op} , the corresponding expression is given by³⁸

$$P_{\text{ac}} = -\frac{gD^2}{8\pi^3 \rho_m \hbar^7 n_e v_F^4 v_s^4} \int_0^\infty dE_k \times \int_0^{\hbar\omega_q^m} d(\hbar\omega_q) (\hbar\omega_q)^3 \frac{(E_k + \hbar\omega_q)^2}{|\epsilon(q, T)|^2} \chi(q, k) \times [N_q(T_e) - N_q(T)] [f(E_k) - f(E_k + \hbar\omega_q)], \quad (18)$$

where D is the acoustic phonon deformation potential coupling constant, v_s is the acoustic phonon velocity, ρ_m is the mass density, $\chi(q, k) = 1 - q^2/(4k^2)$, $\omega_q = v_s q$, and $\omega_q^m = 2v_s k$. The temperature dependent screening function is given by $\epsilon(q, T) = 1 + \Pi(q, T)$, where $\Pi(q, T)$ is the finite temperature static polarizability, evaluated explicitly in Ref.[24].

F. Hot electron cooling power due to optical phonons in 3D semiconductor

With a view to compare the results of the 3DDS Cd₃As₂ with those in 3D Cd₃As₂ semiconductor, we give the expression for the P_{op} for a 3DEG in bulk Cd₃As₂ semiconductor. Taking the parabolic energy relation $E_k = \hbar^2 k^2 / (2m^*)$ (m^* is the effective mass of electron), it is given by

$$P_{op} = \frac{m^{*\frac{3}{2}} \omega_0}{\sqrt{2\pi^2 n_e \hbar^2}} \int_0^\infty dE_q E_q^{\frac{1}{2}} \times [(N_q + 1)e^{-\beta_e \hbar \omega_0} - N_q] \Gamma_q. \quad (19)$$

In this case $E_q = \hbar^2 q^2 / (2m^*)$. The corresponding el-ph scattering rate Γ_q is given by

$$\Gamma_q = g \frac{V m^{*\frac{3}{2}} |g(q)|^2}{2^{\frac{3}{2}} \pi \hbar^4 E_q^{\frac{1}{2}}} \int_{E_k^l}^\infty dE_k f(E_k) [1 - f(E_k + \hbar \omega_0)], \quad (20)$$

where $E_k^l = (\hbar \omega_0 - E_q)^2 / (4E_q)$.

G. Electron energy relaxation time

Some times it is useful to study the hot electron relaxation in terms of corresponding relaxation time τ_e , given by⁴¹ $\tau_e = [\langle E_k(T_e) \rangle - \langle E_k(T) \rangle] / P$ where $\langle E_k(T_e) \rangle = (1/N_e) \int E_k f(E_k) D(E_k) dE_k$ is the average energy of the electron at temperature T_e . For large electron density and very low temperature, expressing density of states $D(E_k) = D_0 E_k^p$, we find

$$\langle E_k(T_e) \rangle = \frac{p+1}{p+2} E_F \left[1 + \frac{(p+2)}{6} \left(\frac{\pi k_B T_e}{E_F} \right)^2 \right], \quad (21)$$

where E_F is the Fermi energy at $T_e=0$. This formula is applicable to 3D and 2D fermions and Dirac fermions with the respective choice of E_F and p .

III. RESULTS AND DISCUSSIONS

In the following, we numerically study the hot phonon distribution and electron cooling power in 3D Dirac semimetal Cd₃As₂ in the range for electron temperature $T_e = (5-300)$ K and electron density $n_e = (0.1-3)n_0$, where $n_0 = 1.0 \times 10^{24} \text{ m}^{-3}$, taking the lattice temperature

$T=4.2$ K. In addition, we present some results of acoustic phonon limited hot electron cooling power in Cd₃As₂. For comparison we also highlight on the electron cooling power in conventional 3DEG. The values of the parameters appropriate for numerical calculations are given in Table I.

Parameter	Symbol	Value
Lattice constant	a	4.6 Angstrom
Effective mass of electron ³⁹	m^*	$0.036m_e$
Mass density of ion	ρ	$7 \times 10^3 \text{ Kg/m}^3$
Degeneracy		
For 3DDS	g	4
For 3DEG	g	2
Sound velocity	v_s	$2.3 \times 10^3 \text{ m/s}$
Fermi velocity ³⁷	v_F	10^6 m/s
Deformation potential ³⁹	D	20 eV
Optical phonon energy ^{14,40}	$\hbar \omega_0$	25 meV
<hr/>		
Dielectric constant(High Freq.)	ϵ_∞	12
Dielectric constant(Static)	ϵ_0	36
Electron density	n_e	$(0.1-3)n_0$,
Lattice temperature	T	4.2 K
Electron temperature	T_e	(5-300)K

TABLE I: Numerical values of the parameters used for calculation. Note that the knowledge of the lattice constant a is required to calculate $\Pi(q, T)$, given in Ref. [24].

Hot phonon distribution N_q as a function of q is shown for different τ_p , n_e , and T_e , respectively, in Fig. 1 for 3DDS Cd₃As₂. In all the three figures we notice that N_q varies considerably and this q dependence is determined by Γ_q arising from the electron-optical phonon interaction in Eq.(16). Each curve has a broad maximum for about $q = 3.98 \times 10^7 \text{ m}^{-1}$ where the phonon heating is found to be significant. This corresponds to the phase matching phonon wave vector $q_0 = 3.79 \times 10^7 \text{ m}^{-1}$ given by $\hbar v_F q_0 = \hbar \omega_0$. The initial steep increase of N_q may be attributed to the lower limit of E_k integration in the Eq.(16). After a broad maximum, with further increase of q , the N_q is found to decrease first very slowly and then gradually to zero. Similar observations are made in GaAs heterojunctions⁴², bilayer graphene⁴³ and monolayer MoS₂³⁵. Writing N_q as the hot phonon number $N_q(T_{ph})$ given by Bose distribution at an effective hot phonon temperature T_{ph} , it can be shown from Eq. (10) that, for $\Gamma_q \gg \tau_p^{-1}$, $T_e \gg T$, and $\beta_e \sim (\hbar \omega_0)^{-1}$ the $N_q(T_{ph})$ approaches the $N_q(T_e)$.

In Fig. 1(a), N_q vs q is shown for different $T_e = 50, 100, 200,$ and 300 K with $n_e = n_0$ and $\tau_p = 5$ ps. The phonon number N_q increases with increasing T_e , as expected on the physical ground that electrons with larger T_e can emit large number of phonons. The N_q corresponding to $T_e = 50$ K is very small compared to the other T_e values, with largest value of $N_q \simeq 0.6$ corresponding to 300K. The width of the maximum is larger for smaller T_e , similar to the findings in monolayer MoS₂³⁵.

N_q dependence on phonon relaxation time τ_p is shown

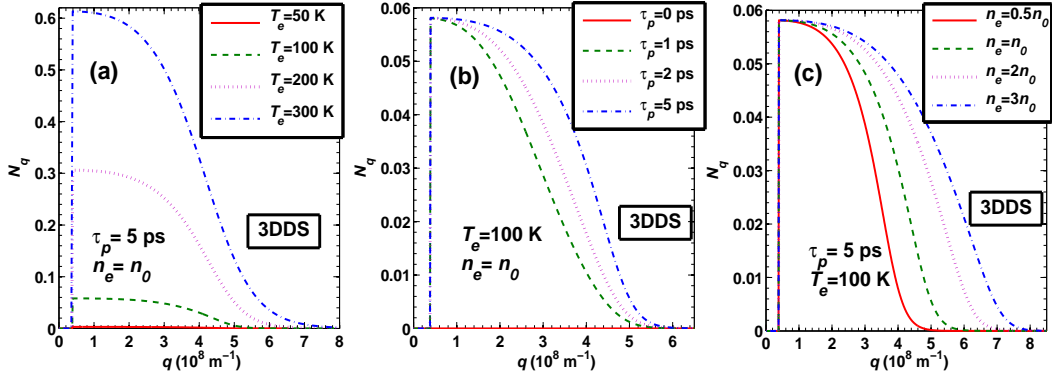


FIG. 1: Non-equilibrium distribution of polar optical phonon N_q in 3DDS Cd_3As_2 as a function function of phonon wave vector q for different T_e , τ_p , and n_e .

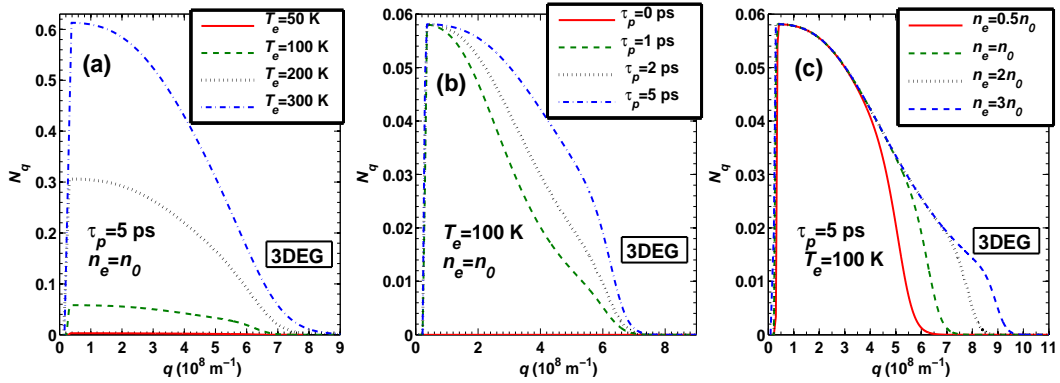


FIG. 2: Non-equilibrium distribution of polar optical phonon N_q in 3DEG Cd_3As_2 semiconductor as a function function of phonon wave vector q for different T_e , τ_p , and n_e .

in Fig. 1(b) by plotting N_q vs q for $\tau_p = 0, 1, 2,$ and 5 ps with $n_e = n_0$ and $T_e = 100$ K. Number of hot phonons is found to be larger for larger relaxation time, as anticipated. Secondly, we notice that the range of q for which N_q remains maximum and nearly constant (i.e. width of the maximum) is larger for phonons with larger τ_p .

The effect of n_e on hot phonon distribution is shown in Fig. 1(c) for $\tau_p = 5$ ps at $T_e = 100$ K. The electron density chosen are $n_e = 0.5n_0, n_0, 2n_0,$ and $3n_0$. N_q is found to be larger for larger n_e because larger density of electrons emit large number of phonons. Moreover, width of the maximum is larger for larger n_e . Similar observation is made in GaN/AlGaIn heterostructure⁴⁴.

For comparison we have shown N_q vs q , in Fig. 2 for different T_e , τ_p , and n_e for 3DEG in bulk Cd_3As_2 semiconductor. We see that maximum of N_q in this semiconductor is almost same as found for 3DDS Cd_3As_2 for each of the T_e . But, unlike in 3DDS Cd_3As_2 , this maximum is spread over relatively a small range of q . The maximum occurs around $q \sim 1 \times 10^8 \text{ m}^{-1}$ which is closer to the phase matching value of $q_0 = (2m\omega_0/\hbar)^{1/2} = 1.54 \times 10^8 \text{ m}^{-1}$. In the low q region N_q increases rapidly with q , and after reaching the maximum it gradually decreases.

Finally it vanishes at relatively larger q values as compared to 3DDS. From Fig. 2(c), in which N_q is shown for different n_e , we see that, for Cd_3As_2 semiconductor N_q remains same, unlike the case of 3DDS Cd_3As_2 (Fig. 1c), for certain range of q for all n_e . Beyond this, N_q is found to be larger for larger n_e at larger q .

In Fig. 3(a), we have shown electron cooling power P_{op} , due to optical phonons, as a function of T_e for different phonon relaxation time $\tau_p = 0, 1, 2,$ and 5 ps. The curve for $\tau_p = 0$ ps corresponds to P_{op} without hot phonon effect. In low T_e (about < 50 K), all the curves show rapid increase of P_{op} with T_e . This is expected because in low T_e region $\hbar\omega_0/(k_B T_e)$ is large and it decreases significantly with increase of T_e . Consequently the optical phonon emission increases as $\sim \exp(-\hbar\omega_0/(k_B T_e))$. In the higher T_e region, P_{op} increases slowly. This behavior may be approximately put as $\exp(-\hbar\omega_0/(k_B T_e))$ attributing to the exponential growth of occupation of electron states with high enough energy to emit optical phonons. At $T_e = 300$ K, the $\hbar\omega_0/(k_B T_e)$ is nearly 1 and P_{op} is nearly constant.

We find that the hot phonon effect reduces P_{op} significantly. However, the hot phonon effect is larger for $\tau_p < 1$

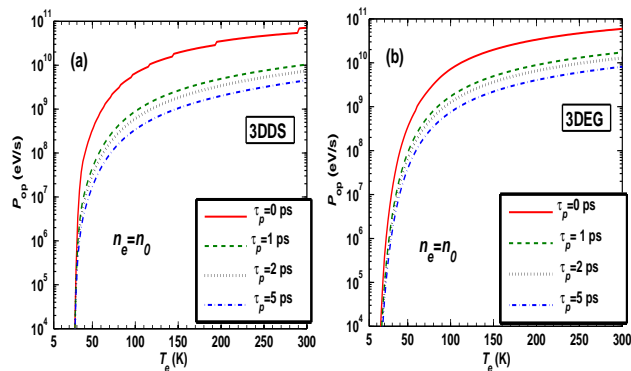


FIG. 3: Temperature dependence of P_{op} for different values of τ_p at $n_e=n_0$. Left and right panels show the results corresponding to 3DDS Cd₃As₂ and for 3DEG in Cd₃As₂ semiconductor, respectively.

ps and smaller for higher values of τ_p . We can introduce a reduction factor $R_{op} = P_{op}(\text{without hot phonon effect})/P_{op}(\text{with hot phonon effect})$, which is always expected to be greater than 1. The reduction factor increases with increasing τ_p , as expected, because there is increased number of hot phonons for larger τ_p which are partially reabsorbed and hence reducing the further electron power loss. For example, for $\tau_p=1$ ps, at $T_e=100$ and 300 K, the reduction factors are $R_{op}=7.37$ and 6.86, respectively. For $\tau_p=5$ ps, at $T_e=100$ and 300 K, the reduction factors, respectively, are $R_{op}=19.21$ and 15.72. This observation indicates that hot phonon effect is sensitive at low T_e and less sensitive at higher T_e .

For comparison, P_{op} is shown as a function of T_e , in Fig. 3(b), for 3DEG in Cd₃As₂ semiconductor for $\tau_p = 0, 1, 2, \text{ and } 5$ ps. It is found that without hot phonon effect (i.e $\tau_p=0$), P_{op} in 3DEG is much larger than that in 3DDS in the temperature regime $T_e < 30$ K. Above $T_e \sim 40$ K, the corresponding values of P_{op} are almost same. With hot phonon effect ($\tau_p \neq 0$), P_{op} in 3DEG is larger than P_{op} in 3DDS over the entire range of temperature considered. The difference between the values of P_{op} in 3DEG and 3DDS is huge below $T_e \sim 30$ K. However, this difference above $T_e \sim 40$ K is small and it is increasing with τ_p . In Cd₃As₂ semiconductor, we find for $\tau_p=1$ ps at $T_e=100(300)$ K, $R_{op}=4.17(3.44)$. For $\tau_p=5$ ps, it is obtained $R_{op}=9.52(7.29)$ at $T_e=100(300)$ K. These values of R_{op} are smaller than that found in 3DDS. This larger reduction of P_{op} in 3DDS Cd₃As₂ indicates that, at a given T_e , hot phonon population is more in this system compared to 3D Cd₃As₂ semiconductor. This can be seen from the more broader maximum of N_q in the former system.

In Fig. 4(a)(4(b)) P_{op} is shown as a function of T_e for different n_e in 3DDS (3DEG) Cd₃As₂ taking $\tau_p=5$ ps. In 3DDS Cd₃As₂ (Fig. 4(a)) P_{op} is found to be smaller for larger n_e . For about $T_e < 50$ K, P_{op} is found to be more sensitive to n_e and the dependence becomes weaker at

higher T_e . However, the situation is different for 3DEG in Cd₃As₂ semiconductor. As depicted in Fig. 4(b) the n_e sensitivity of P_{op} is more in high T_e regime than that in low T_e range.

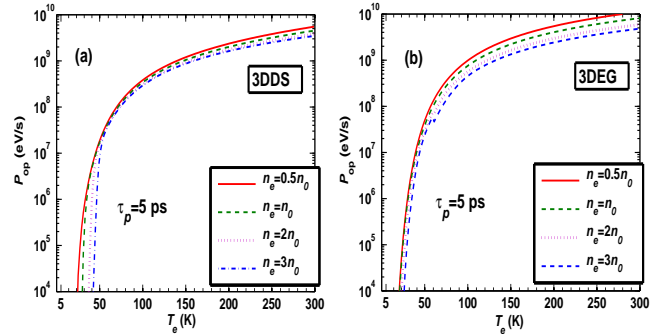


FIG. 4: Temperature dependence of P_{op} for different values of n_e at $\tau_p=5$ ps. Left and right panels show the results corresponding to 3DDS Cd₃As₂ and for 3DEG in Cd₃As₂ semiconductor, respectively.

In Fig. 5, we show temperature dependence of hot electron cooling power due to acoustic phonons P_{ac} and optical phonons P_{op} considering hot phonon effect (with $\tau_p=5$ ps) as well as the total $P_T=P_{op}+P_{ac}$. P_{ac} increases superlinearly in low T_e region and then approaches $\sim T_e$, which is generic at higher T_e . It is also found that, in this temperature range, P_{ac} is smaller for smaller n_e , unlike the case of P_{op} . In Fig. 5(b), we see that there is a crossover from acoustic phonon to optical phonon dominated cooling power. The T_e at which the crossover takes place depends upon n_e significantly. It is found that crossover takes place at $T_e \sim 25, 30, 39, \text{ and } 45$ K for $n_e=0.5n_0, n_0, 2n_0, \text{ and } 3n_0$, respectively. Optical phonon is the active channel of power dissipation above this T_e . The crossover temperature may depend on τ_p also. Considering $n_e=0.5n_0$, the crossover $T_e=25$ K may be compared with about 20 K in InSb²⁷ and 35 K in GaAs^{28,30} bulk semiconductors noting that these samples are non-degenerate. The $T_e=25$ K above which P_{op} is dominating P_T in Cd₃As₂ is closer to that in bulk InSb as optical phonon energies in these two systems are closer. It is to be noted that in InSb(GaAs) $\hbar\omega_0$ is 24.4(36.5) meV. In the neighborhood of cross over T_e , P_T shows a knee like behavior as found in InSb²⁷ and GaAs²⁸.

In the Bloch-Grüneisen (BG) regime, $T_e \ll T_{BG}=(2\hbar v_s k_F/k_B)$, where k_F is the Fermi wave vector, the P_{ac} dependence on T_e and n_e are shown to be given by the power laws $P_{ac} \sim T_e^\alpha$ and $n_e^{-\delta}$ where $\alpha=9(5)$ and $\delta=5/3(1/3)$ with(without) screening of electron-acoustic phonon interaction³⁸. In relatively higher $T_e (> T_{BG})$ regime, disorder assisted P_{ac} calculations show drastic increase of cooling power due to enhanced energy transfer between electrons and acoustic phonons³⁷.

In Fig. 6(a) (6(b)) P_{op} is shown as a function of T_e for different T_e in 3DDS (3DEG) Cd₃As₂ taking $\tau_p=5$ ps. In 3DDS Cd₃As₂, P_{op} is found to decrease weakly

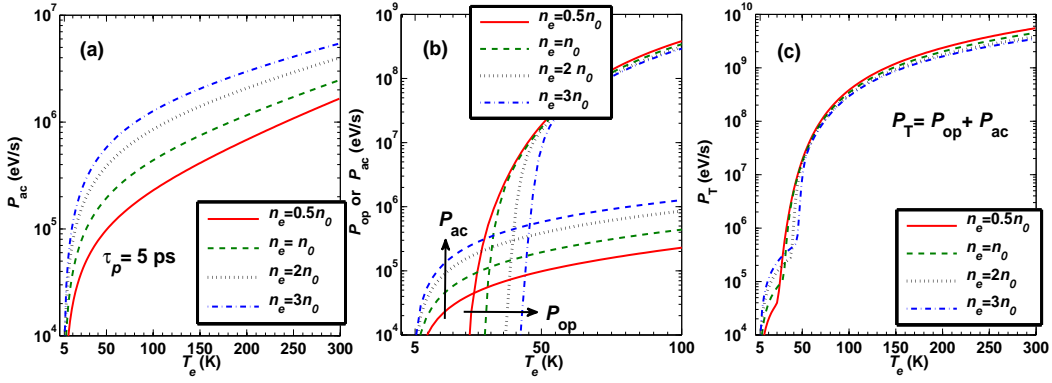


FIG. 5: Temperature dependence of P_{ac} and P_{op} in 3DDS Cd_3As_2 for different values of n_e . (a) P_{ac} in the range $T_e=5-300$ K, (b) P_{ac} and P_{op} in the range $T_e=5-100$ K and (c) $P_T=P_{ac} + P_{op}$. Note that P_{op} is for $\tau_p=5$ ps.

with increasing n_e . This decrease may be attributed to partial reabsorption of large number of phonons emitted by larger n_e . The decrease is, relatively, faster (slower) at low (high) n_e . Moreover, it is found that, compared to 3DEG in Cd_3As_2 semiconductor (Fig. 6(b)), P_{op} in 3DDS Cd_3As_2 is less sensitive to n_e . This may be attributed to differing density of states. For example, while varying n_e from $0.1n_0$ to $3n_0$ P_{op} decreases, at $T_e=300$ K, by a factor of about 2.75(5) in 3DDS (3DEG) Cd_3As_2 . At $T_e=100$ K the respective changes are 1.82 and 4.29.

spectively. Consequently, taking $P_{op}=3.417(45.364) \times 10^8$ eV/s at $T_e=100(300)$ K we find energy relaxation time $\tau_e=6.73(4.21)$ ps. Alternatively, τ_e can be obtained from $1/\tau_e = (1/C_e)(dP/dT_e)$, where C_e is the electronic heat capacity. However, simple power laws can be obtained in BG regime, where P_{ac} is the sole contributor to electron cooling power, with regard to T_e and n_e dependence. Using the BG regime results, we find $\tau_e \sim T_e^{-7}(T_e^{-3})$ and $n_e^{4/3}(n_0^0)$ for screened (unscreened) electron-acoustic phonon interaction.

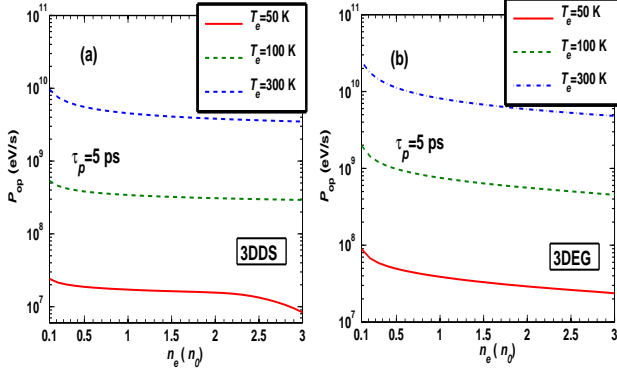


FIG. 6: Density dependence of P_{op} in 3DDS Cd_3As_2 and for 3DEG in Cd_3As_2 semiconductor for different temperatures. Hot phonon effect is taken into account with $\tau_p=5$ ps.

Electron cooling power due to optical phonons in bulk GaAs is shown to be reduced by screening effect²⁹. In 3DDS Cd_3As_2 also we expect the screening to reduce P_{op} . Although screening effect is not considered in our P_{op} calculations, the experimental measurements will be able to indicate its necessity.

We would like to mention that our numerical calculations of P can be used to calculate energy relaxation time τ_e as given in section II(G). For $n_e=n_0$, the average electron energy is found to be $\langle E(T_e) \rangle = 0.1212, 0.1235,$ and 0.1403 eV at $T_e=4.2, 100,$ and 300 K, re-

IV. SUMMARY

In summary, we have studied optical phonon limited cooling of hot electrons in 3DDS Cd_3As_2 considering the effect of hot phonon. The dependence of electron cooling power P_{op} , due to optical phonon, on electron temperature T_e , electron density n_e , and phonon relaxation time τ_p are investigated. P_{op} is found to increase much rapidly with T_e at low temperature regime while this increase becomes much slower in high T_e regime. The dependence of P_{op} on n_e is weak. It shows a slow decrease with the increase of n_e . We compare the results with those corresponding to 3DEG in Cd_3As_2 semiconductor. It is revealed that hot phonon effect is stronger in 3DDS Cd_3As_2 than in Cd_3As_2 semiconductor. It is also found that P_{op} is more (less) sensitive to n_e in 3DEG (3DDS). Additionally, P_{op} is compared with the acoustic phonon limited hot electron cooling power P_{ac} . A crossover from P_{ac} dominated cooling at low T_e to P_{op} dominated cooling at higher T_e takes place at about $T_e=25$ K for $n_e=0.5n_0$. The crossover T_e shifts towards higher temperature for larger n_e . We point out that our calculations need to be tested against the experimental data. We suggest for steady state/electric field experiments in n -type 3DDS Cd_3As_2 to which our present calculations will be directly related.

- * Electronic address: sskubakaddi@gmail.com
- † Electronic address: tbtutulum53@gmail.com
- ¹ Z. Wang, Y. Sun, X. Q. Chen, C. Franchini, G. Xu, H. Weng, X. Dai, and Z. Fang, *Phys. Rev. B* **85**, 195320 (2012).
 - ² Z. Wang, H. Weng, Q. Wu, X. Dai, and Z. Fang, *Phys. Rev. B* **88**, 125427 (2013).
 - ³ S. Borisenko, Q. Gibson, D. Evtushinsky, V. Zabolotnyy, B. Büchner, and R. J. Cava, *Phys. Rev. Lett.* **113**, 027603 (2014).
 - ⁴ Z. K. Liu, J. Jiang, B. Zhou, Z. J. Wang, Y. Zhang, H. M. Weng, D. Prabhakaran, S-K. Mo, H. Peng, P. Dudin, T. Kim, M. Hoesch, Z. Fang, X. Dai, Z. X. Shen, D. L. Feng, Z. Hussain, and Y. L. Chen *Nat. Mater.* **13**, 677 (2014).
 - ⁵ M. Neupane, S.-Y. Xu, R. Sankar, N. Alidoust, G. Bian, C. Liu, I. Belopolski, T. R. Chang, H. T. Jeng, H. Lin, A. Bansil, F. Chou, and M. Z. Hasan *Nat. Commun.* **5**, 3786 (2014).
 - ⁶ S. Jeon, B. B. Zhou, A. Gyenis, B. E. Feldman, I. Kimchi, A. C. Potter, Q. D. Gibson, R. J. Cava, A. Vishwanath, and A. Yazdani *Nat. Mater.* **13**, 851 (2014).
 - ⁷ L.P. He, X.C. Hong, J.K. Dong, J. Pan, Z. Zhang, J. Zhang, and S.Y. Li, *Phys. Rev. Lett.* **113**, 246402 (2014).
 - ⁸ Z. K. Liu, B. Zhou, Y. Zhang, Z. J. Wang, H. M. Weng, D. Prabhakaran, S-K. Mo, Z. X. Shen, Z. Fang, X. Dai, Z. Hussain, and Y. L. Chen, *Science* **343**, 864 (2014).
 - ⁹ T. Liang, Q. Gibson, M. N. Ali, M. Liu, R. J. Cava, and N. P. Ong, *Nat. Mater.* **14**, 280 (2015).
 - ¹⁰ Y. Zhao, H. Liu, C. Zhang, H. Wang, J. Wang, Z. Lin, Y. Xing, H. Lu, J. Liu, Y. Wang, S. M. Brombosz, Z. Xiao, S. Jia, X.C. Xie, and J. Wang, *Phys. Rev. X* **5**, 031037 (2015).
 - ¹¹ C. P. Weber, E. Arushanov, B. S. Berggren, T. Hosseini, N. Kouklin, and A. Nateprov, *Appl. Phys. Lett.* **106**, 231904 (2015).
 - ¹² H. Weng, X. Dai, and Z. Fang, *J. Phys. : Conds. Matt.* **28**, 303001 (2016).
 - ¹³ Q. Wang, C. Z. Li, S. Ge, J. G. Li, W. Lu, J. Lai, X. Liu, J. Ma, D. P. Yu, Z. M. Liao, and D. Sun, *Nano Lett.* **17**, 834 (2017).
 - ¹⁴ W. Lu, S. Ge, X. Liu, H. Lu, C. Li, J. Lai, C. Zhao, Z. Liao, S. Jia, and D. Sun, *Phys. Rev. B* **95**, 024303 (2017).
 - ¹⁵ C. Zhu, X. Yuan, F. Xiu, C. Zhang, Y. Xu, R. Zhang, Y. Shi and F. Wang, *Appl. Phys. Lett.* **111**, 091101 (2017).
 - ¹⁶ C. P. Weber, B. S. Berggren, M. G. Masten, T. C. Ogloza, S. Deckoff-Jones, J. Madeo, M. K. L. Man, K. M. Dani, L. Zhao, G. Chen, J. Liu, Z. Mao, L. M. Schoop, B. V. Lotsch, S. S. P. Parkin, and M. Ali, *J. Appl. Phys.* **122**, 223102 (2017).
 - ¹⁷ C. Zhu, F. Wang, Y. Meng, X. Yuan, F. Xiu, H. Luo, Y. Wang, J. Li, X. Lv, L. He, Y. Xu, J. Liu, C. Zhang, Y. Shi, R. Zhang, and S. Zhu, *Nat. Commun.* **8**, 14111 (2017).
 - ¹⁸ J. Feng, Y. Pang, D. Wu, Z. Wang, H. Weng, J. Li, X. Dai, Z. Fang, Y. Shi, and L. Lu *Phys. Rev. B* **92**, 081306 (2015).
 - ¹⁹ A. Narayanan, M.D. Watson, S.F. Blake, N. Bruyant, L. Drigo, Y.L. Chen, D. Prabhakaran, B. Yan, C. Felser, T. Kong, P.C. Canfield, and A.I. Coldea *Phys. Rev. Lett.* **114**, 117201 (2015).
 - ²⁰ H. Li, H. He, H. Z. Lu, H. Zhang, H. Liu, R. Ma, Z. Fan, S. Q. Shen, and J. Wang, *Nat. Comm.* **7**, 10301 (2016).
 - ²¹ Z. G. Chen, C. Zhang, Y. Zou, E. Zhang, L. Yang, M. Hong, F. Xiu, and J. Zou, *Nano Lett.* **15**, 5830 (2015).
 - ²² E. Zhang, Y. Liu, W. Wang, C. Zhang, P. Zhou, Z. Chen, J. Zou and F. Xiu, *ACS Nano* **9**, 8843 (2015)
 - ²³ R. Lundgren, P. Laurell, and G. A. Fiete, *Phys. Rev. B* **90**, 165115 (2014).
 - ²⁴ S. Das Sarma, E. H. Hwang, and H. Min, *Phys. Rev. B* **91**, 035201 (2015).
 - ²⁵ E. M. Conwell, *High field transport in semiconductors* (Academic, New York, 1967).
 - ²⁶ K. Seeger, *Semiconductor Physics: An Introduction*, Springer Series in Solid State Sciences, 9th ed. (Springer-Verlag, Berlin Heidelberg, 2004).
 - ²⁷ J. R. Sandercock, *Proc. Phys. Soc.* **86**, 1221 (1965); J. P. Maneval, A. Zylbersztejn, and H. F. Budd, *Phys. Rev. Lett.* **23** 848 (1969); S. S. Kubakaddi and B. S. Krishnamurthy, *Phys. Lett. A* **54**, 389 (1975); K. Shimomae, Y. Hirose and C. Hamaguchi, *J. Phys. C: Solid State Phys.*, **14**, 5151 (1981).
 - ²⁸ K. Hess and H. Kahlert, *J. Phys. Chem. Solids* **32**, 2262 (1971); S. S. Kubakaddi and B. G. Mulimani, *Phys. Lett. A* **103**, 141 (1984).
 - ²⁹ S. D. Sarma, J. K. Jain, and R. Jalabert, *Phys. Rev. B* **37**, 6290 (1988).
 - ³⁰ S. S. Prabhu, A. S. Vengurlekar, S. K. Roy, and J. Shah, *Phys. Rev. B* **51**, 14233 (1995).
 - ³¹ B. K. Ridley, *Rep. Prog. Phys.* **54**, 169 (1991).
 - ³² P. J. Price, *J. Appl. Phys.* **53**, 6863 (1982); J. Shah, A. Pinczuk, A. C. Gossard, and W. Wiegmann, *Phys. Rev. Lett.* **54**, 2045 (1985); S. J. Manion, M. Artaki, M. A. Emanuel, J. J. Coleman and K. Hess, *Phys. Rev. B* **35**, 9203 (1987); S. Das Sarma, J. K. Jain and R. Jalabert, *Phys. Rev. B* **37**, 1228 (1988); Y. Ma, R. Fletcher, E. Zaremba, M. DiIorio, C. T. Foxon, and J. J. Harris, *Phys. Rev. B* **43**, 9033 (1991); S. S. Kubakaddi, K. Suresha, and B. G. Mulimani, *Semicond. Sci. Technol.* **17**, 557 (2002).
 - ³³ S. S. Kubakaddi, *Phys. Rev. B* **79**, 075417 (2009); R. Bistrizter and A. H. MacDonald, *Phys. Rev. B* **80**, 085109 (2009); J. K. Viljas and T.T. Heikkila, *Phys. Rev. B* **81**, 245404 (2010); A. C. Betz, et al., *Phys. Rev.Lett.* **109**, 056805 (2012); J. C. W. Song, M. Y. Reizer, and L. S. Levitov, *Phys. Rev. Lett.* **109**, 106602 (2012); A. M. R. Baker et al., *Phys. Rev. B* **87**, 045414 (2013). R. Somphonsane, et al., *Nano Lett.* **13**, 4305 (2013); W. Song, L.S. Levitov, *J. Phys.: Condens. Matter* **27**, 164201(2015).
 - ³⁴ K. S. Bhargavi and S. S. Kubakaddi, *Physica E* **56**, 123 (2014); J. Huang et al., *J. Phys.: Condens. Matter* **27**, 164202 (2015); A. Laitinen et al., *Phys. Rev. B* **91**, 121414(R) (2015); S. S. Kubakaddi, *Physica E* **95**,144 (2018).
 - ³⁵ K. Kaasbjerg, K. S. Bhargavi, and S. S. Kubakaddi, *Phys. Rev. B* **90**, 165436 (2014).
 - ³⁶ S. Huang, M. Sanderson, J. Tian, Q. Chen, F. Wang, and C. Zhang, *J. Phys. D: Appl. Phys.* **51**, 015101 (2018).
 - ³⁷ R. Lundgren and G. A. Fiete, *Phys. Rev. B* **92**, 125139 (2015).
 - ³⁸ K. S. Bhargavi and S. S. Kubakaddi, *Phys. Staus Solidi RRL* **10**, 248 (2016). **In this paper a typo error $\rho\pi^2$ to be deleted in the denominator of r.h.s of Eq.(1)**
 - ³⁹ J. P. Jay-Gerin, M. J. Aubin and L. G. Caron, *Phys. Rev. B* **18**, 4542 (1978).

- ⁴⁰ J. Weszka, Phys. Stat. Sol. (b) **211**, 605 (1999).
- ⁴¹ B. K. Ridley, Quantum Processes in Semiconductors, 2nd edition, Oxford science Publications,(Clarendon Press, Oxford, 1988), p. 327.
- ⁴² J. Z. Zhang, B. F. Zhu, and J. Huang, Phys. Rev. B **59**, 13184 (1999).
- ⁴³ V. S. Katti and S. S. Kubakaddi, J. Appl. Phys. **113**, 063705 (2013).
- ⁴⁴ S. Gokden, N. Balkan, and B. K. Ridley, Semicond. Sci. Technol. **18**, 206 (2003).